Limnol. Oceanogr., 52(1), 2007, 257 273

A time series of environmental tracer data from deep, meromictic Lake Lugano, Switzerland

W. Aeschbach-Hertig
Institute of Environmental Physics, University of Heidelberg, D-69120 Heidelberg, Germany

C. P. Holzner
Water Resources and Drinking Water, Swiss Federal Institute of Aquatic Science and Technology (Eawag), CH-8600 Dübendorf, Switzerland; Environmental Physics, Swiss Federal Institute of Technology (ETH), CH-8902 Zurich, Switzerland

M. Hofer
Water Resources and Drinking Water, Swiss Federal Institute of Aquatic Science and Technology (Eawag), CH-8600 Dübendorf, Switzerland

M. Simona and A. Barbieri
Ufficio Protezione e Depurazione Acque, Sezione Protezione Aria, Acqua e Suolo, Dipartimento del Territorio, Cantone Ticino CH 6500 Bellinzona, Switzerland

R. Kipfer
Water Resources and Drinking Water, Swiss Federal Institute of Aquatic Science and Technology (Eawag), CH-8600 Dübendorf, Switzerland; Isotope Geology, Swiss Federal Institute of Technology (ETH), CH-8902 Zurich, Switzerland

Abstract

An 11 yr (1990 2001) time series of tritium helium 3 (^{3}H ^{3}He) apparent water ages as well as one sulfur hexafluoride (SF_6) profile were used to study the development of the vertical mixing dynamics of the deep, meromictic northern basin of Lake Lugano. The density stratification of the water column was dominated by an increase in dissolved ions with depth, which remained approximately constant during the 1990s. The deep water temperature increased steadily during this period, passing a threshold above which cooling of the surface water could force convection. However, increasingly mild winter temperatures prevented the occurrence of a turnover until 2005. The maximum apparent ^{3}H ^{3}He water age increased from about 16 yr in 1990 to 23 yr in 2001. The maximum apparent SF_6 age in 2001 was 12.8 yr. The large difference between the apparent ^{3}H ^{3}He and SF_6 ages is at least partly due to nonlinear effects of mixing, causing SF_6 ages to underestimate the true mean deep water residence time, whereas ^{3}H ^{3}He ages overestimate it. The decreasing concentrations of ^{3}H and ^{3}He are more reliable indicators of the continuous deep water exchange in the lake than are the apparent ages. Budget calculations using the tracer concentrations reveal an annual renewal of the deep water below 100 m in depth by about 8% and enable the calculation of long term mean profiles of the effective vertical turbulent diffusivity K_z. No trend in the mixing intensity during the 1990s could be determined. The radiogenic He flux into the lake is comparable to estimates of the whole crustal degassing flux.

Lake Lugano is a deep perialpine lake, which, as a result of eutrophication during the second half of the last century, experienced a serious deterioration of water quality, in particular a complete and enduring anoxia in the deep water below about 100 m in depth (Barbieri and Mosello 1992). Although the inflow of nutrients has been reduced and the water quality of the surface water has improved during the last decades, the regeneration of the deep water body has been a very slow process, impaired by sluggish vertical mixing due to a chemical stratification of the water column (Wüest et al. 1992). A thorough understanding of the mixing dynamics of the lake, including the response to changing biogeochemical and climatic conditions, is therefore important for the management of the lake.

Transient environmental tracers such as the tritium-helium-3 (^{3}H-^{3}He) isotope pair or chlorofluorocarbons (CFCs) have proved to be excellent tools for studying the mixing dynamics of lakes (e.g., Torgersen et al. 1977; Weiss et al. 1991; Aeschbach-Hertig et al. 1996). The methods are

Acknowledgments

We thank Urs Beyerle, Matthias Brennwald, Roland Hoh mann, David Livingstone, and Frank Peeters for their respective contributions to the fieldwork, the He and ^{3}H analyses, the preparation of the CTD data, and the improvement of the manuscript. Special thanks go to Dieter Imboden and Alfred Johny Wüest for support and advice in the early phase of the project and to Heiri Baur for always keeping the ETH noble gas lab going over so many years. Two anonymous reviewers provided careful and constructive reviews.

particularly appropriate to study the deep-water renewal in deep meromictic lakes (i.e., lakes that do not undergo an annual full turnover of the water column: e.g., Campbell and Torgersen 1980; Torgersen et al. 1981; Hohmann et al. 1998; Peeters et al. 2000; Aeschbach-Hertig et al. 2002). In addition to the established methods, sulfur hexafluoride (SF_6) has recently been introduced as a promising tracer in hydrology (Busenberg and Plummer 2000) as well as in physical limnology (Hofer et al. 2002; Vollmer et al. 2002).

All these environmental tracers provide direct information on the time passed since the last contact of a water parcel with the atmosphere, the so-called water age. The age information is derived from the transient atmospheric histories of the CFCs and SF_6 and from the buildup of the ^3He concentration as a result of the radioactive decay of ^3H. However, if a water mass experiences mixing, its tracer-derived water age generally deviates from its true mean water age (e.g., Hofer et al. 2002). This is because the tracer input histories as well as the concentration changes due to radioactive decay are nonlinear with time. The effect is most pronounced when waters with large age differences mix, which is the case in lakes when surface water with near-zero age (due to gas exchange) mixes with old deep water. Furthermore, gas exchange may not be able to achieve equilibration of a deep mixed layer, so that the tracer age represents a dissolved gas age rather than a water age. For all of these reasons it is important to distinguish between the apparent tracer ages and the true mean residence time of a mixed water parcel.

Nevertheless, the tracer concentrations still provide useful approximate age information. Wüest et al. (1992) presented the first ^3H-^3He profile from Lake Lugano sampled in 1990, which showed an apparent deep-water age of about 16 yr, demonstrating that deep-water renewal is slow in this lake. However, based on a single tracer profile it is impossible to derive the history of the mixing dynamics in this changing system. In this study, we present a time series of ^3H-^3He data from the northern basin of Lake Lugano that extends from 1990 to 2001 (including the profile from Wüest et al. 1992), accompanied by high-resolution conductivity temperature depth (CTD) profiles. This time series is complemented by SF_6 data from 2001. CFC data from 1996 and 2001 could not be used for age dating because of CFC-12 (CF_2Cl_2) contamination and CFC-11 ($CFCl_3$) degradation.

This database provides a unique opportunity to study the long-term development of the lake's mixing dynamics. In particular, it constitutes a reference for the lake's stagnant state, against which recent changes can be compared. In spring 2005 an unexpected deep mixing event took place in Lake Lugano (SPAAS 2005). The consequences of this mixing, including new tracer data, will be presented elsewhere.

Study area

Lake Lugano (Fig. 1) lies on the southern fringe of the Alps in the Swiss Italian border area (46°00′N, 8°30′E). A short description of the lake was given by Barbieri and Polli (1992); comprehensive data on the hydrology and meteorology of the region as well as the characteristics of the lake can be found in the annual reports of the International Commission for the Protection of Italo Swiss Waters (LSA 1981 2000). The lake is separated into two basins by an artificial dam built on a morainic front. Only the deeper (z_{max} = 288 m) Northern Basin is considered in this study. It can be treated as an individual lake, with the connection to the Southern Basin acting as outflow. The Northern Basin is narrow, elongated, and exceptionally steep. The water input by tributaries is small, resulting in a high hydrological residence time of 12.3 yr ($\tau = V/Q$: volume V = 4.69 km^3, outflow Q = 0.38 km^3 yr $^{-1}$). This theoretical exchange time is of little relevance for the deep water, since mainly the upper ~100 m of the lake (V = 2.36 km^3) are affected by the throughflow. Steep mountains shield the lake from the wind; the average wind speed measured in Lugano in the period ranging from 1971 to 2000 was only 1.7 m s $^{-1}$. The climate is relatively mild, with mean annual air temperatures of 12.0°C and January means of 3.2°C at Lugano for the period ranging from 1971 to 2000 (data from Begert et al. 2005). All these conditions are conducive to slow deep-water renewal as a result of weak forcing by wind, rivers, and winter cooling.

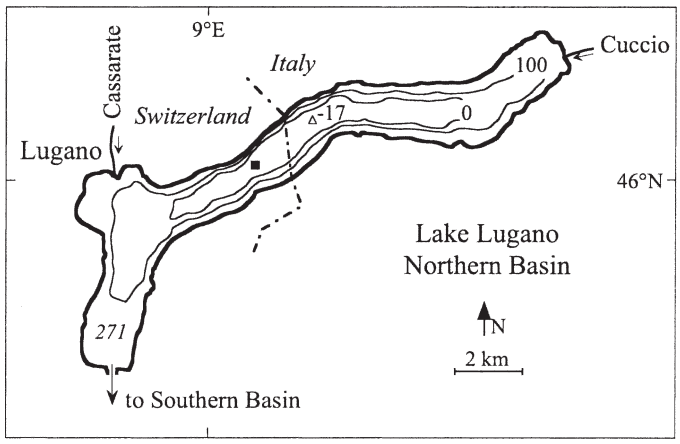

Fig. 1. Map of the northern basin of Lake Lugano. The elevations (above sea level) of the lake surface (271 m), two isobaths at 100 and 0 m (depths of 171 and 271 m), and the deepest point (triangle, 17 m) are indicated. The sampling station (square) is located in the deepest part of the lake.

The unfavorable natural conditions for mixing were aggravated by anthropogenic eutrophication beginning in the 1940s and culminating around 1980, when the concentration of total phosphorus averaged over the entire water column exceeded 150 μg L $^{-1}$ (Barbieri and Mosello 1992). Measures to reduce the phosphorus input started in 1976. In response, phosphorus concentrations in the surface water slowly decreased, whereas in the deep water below 100 m in depth they stabilized at a high level. As a result of the eutrophication, the redox state of the deep water changed dramatically. According to Barbieri and Mosello (1992), oxygen concentrations in the layer below 100 m in depth decreased from 3.5 mg L $^{-1}$ in 1946 to zero in 1960, temporarily increased to 2.2 mg L $^{-1}$ in 1964 as a result of the exceptionally severe winter of 1962 1963, and have permanently remained at zero at least since 1974.

Moreover, the concentrations of reducing substances such as NH_4, H_2S, and CH_4 reached high levels (Barbieri and Simona 2001).

At least since the 1970s and up to 2005, the seasonal convective mixing in Lake Lugano never reached deeper than about 100 m, thus rendering the lake meromictic. Despite this fact, we do not use the term monimolimnion for the water mass below this depth to avoid the misleading impression that this water body is completely isolated. Instead, we will use the terms shallow water for the upper 100 m of the water column, including the well-mixed surface layer and the seasonal thermocline, and deep water for the water body below 100 m in depth.

Wüest et al. (1992) discussed the density structure of the Northern Basin of Lake Lugano and explained its evolution to permanently anoxic conditions based on the increased biological activity in the lake in response to eutrophication, which intensified the flux of organic matter to the deep water. This increased the rate of mineralization, which not only led to strong oxygen depletion but also increased the concentrations of dissolved ions in the deep water, thereby strengthening the density stratification of the water column. Thus, the intensity of deep-water renewal decreased and the oxygenation of the deep water was further reduced. The strength of the winter mixing may have further declined as a result of increasing air temperatures, particularly in winter. Begert et al. (2005) determined warming trends for Lugano from 1864 to 2000 of 0.006°C yr $^{-1}$ for the annual mean and 0.009°C yr $^{-1}$ for the winter months. For the period from 1961 to 2000 the respective trends were much stronger (both ~0.04°C yr $^{-1}$). A major goal of the long-term tracer data series presented here is to study the evolution of the vertical mixing intensity in response to the changing conditions.

Methods

Sampling All sampling for this study took place at a central station in the deepest part of Lake Lugano (square in Fig. 1). Monthly high-resolution CTD profiles have been taken at this station by the Laboratorio Studi Ambientali (LSA) since 1984 (partly published in LSA 1998) using an Idronaut Ocean Seven 501 probe (accuracy of 0.01°C for temperature and 2 μS cm $^{-1}$ for conductivity; resolution of 0.004°C and 0.4 μS cm $^{-1}$, respectively). Additional CTD measurements were performed during the tracer sampling campaigns. In 1990 and 1992, a CTD probe from Meereselektronik GmbH was used (accuracy of 0.01°C, 2 μS cm $^{-1}$; resolution of 0.002°C, 0.2 μS cm $^{-1}$); during the later samplings a Seacat SBE-19 CTD probe (accuracy of 0.01°C, 1 μS cm $^{-1}$; resolution of 0.001°C, 0.01 μS cm $^{-1}$) was employed.

The accuracies given above are initial accuracies stated by the manufacturers of the CTD probes. Since all probes, and especially their conductivity sensors, are subject to small drifts, they were calibrated from time to time. The conductivity profiles taken during the tracer samplings in May 1990 and September 1996 are not used because the correct calibration functions could not be reconstructed. An estimate of the repeatability may be obtained from a comparison of the profiles taken during the tracer samplings with the regular LSA profiles. CTD profiles taken independently within 1 month show maximum deviations of 0.04°C and 15 μS cm $^{-1}$, respectively. While there are offsets in the absolute values, especially for conductivity, the relative shape of all profiles agrees very well.

For the tracer analyses, water samples were taken using Niskin bottles and transferred into gas-tight containers immediately after recovery from the lake. Samples for ^{3}H, noble gas, and CFC analysis were stored in copper tubes that were sealed with stainless-steel clamps on both ends (as described in Beyerle et al. [2000] and Hofer and Imboden [1998]). Water samples for simultaneous determination of SF_6 and CFC-12 were housed in stainless-steel cylinders equipped with two plug valves.

Tracer analyses He isotopes (^{3}He, ^{4}He), Ne, and ^{3}H were analyzed by noble gas mass spectrometry according to the procedures described by Beyerle et al. (2000). Calibration was performed relative to an air standard. The typical 1σ-errors of the samples from Lake Lugano are 0.4% for the ^{3}He : ^{4}He ratios, 0.6% for the ^{4}He concentrations, and 0.8% for the Ne concentrations. These values are close to the long-term mean reproducibility of the system, as derived from regular analyses of aliquots of an internal freshwater standard (Beyerle et al. 2000). The He concentrations from the first sampling (May 1990) have larger uncertainties of about 1.3%. ^{3}H was measured by the ^{3}He ingrowth technique (Clarke et al. 1976). The precision of the ^{3}H measurements is usually a few percent. Some ^{3}H values are missing, either because samples were not analyzed or because they were lost as a result of experimental problems.

CFC-11 and CFC-12 from water samples taken in 1996 were analyzed on a gas chromatograph equipped with an electron capture detector (GC-ECD), according to procedures described by Hofer and Imboden (1998). Samples collected in 2001 were analyzed with a similar method designed for the simultaneous determination of CFC-12 and SF_6. This method also uses a vacuum extraction and purification line and a GC-ECD, but larger samples (0.5 liters) are processed to enable detection of the low SF_6 concentrations. Calibration was performed with a standard gas mixture produced by dilution of commercially available standards with a nominal accuracy of 2% for SF_6. The precision determined from the reproducibility of duplicate water samples with modern concentrations of SF_6 is ±5%. Detection limits are 0.07 and 2 fmol kg $^{-1}$ for SF_6 and CFC-12, respectively.

Calculation of apparent tracer ages The age determination with the tracer pair ^{3}H-^{3}He is based on the radioactive decay of the radioactive hydrogen isotope tritium (^{3}H, half-life 4,500 d = 12.32 yr; decay constant λ = 0.05626 yr $^{-1}$; Lucas and Unterweger 2000) to the stable helium isotope ^{3}He. ^{3}H concentrations in precipitation exhibited a sharp peak in 1963 as a result of thermonuclear weapons tests in the atmosphere. The ^{3}H observation station closest to Lake Lugano is located in Locarno, about 20 km to the northwest. Data from Locarno are available for the period from 1973 to 1992 in the GNIP database (IAEA/WMO

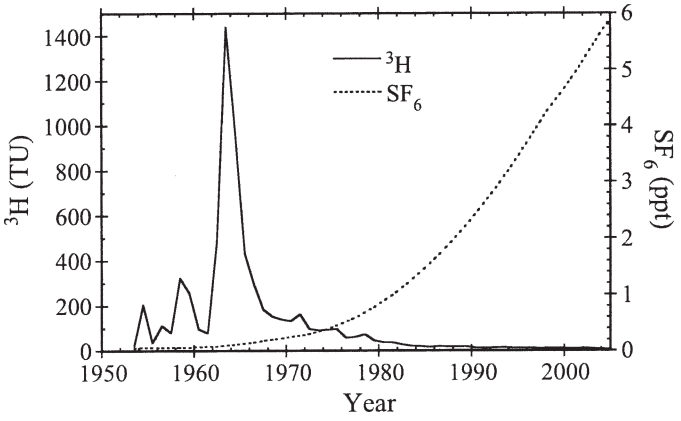

Fig. 2. Input histories of ^{3}H and SF_6. The ^{3}H data are yearly mean concentrations in precipitation at Locarno from 1973 to 2005, extended backwards to 1953 by correlation with data from Vienna and Ottawa. The SF_6 data are atmospheric background mixing ratios taken from IAEA (2006).

2004). Later data (1993 2005) were taken from yearly reports of the Swiss Federal Office of Public Health (DRP 1994 2006). Figure 2 shows the entire record, extended back to 1953 by correlations with data from long-term stations in Vienna and Ottawa, according to procedures used by IAEA (1992).

The apparent ^{3}H-^{3}He water age τ_{3He} is calculated from the concentrations of ^{3}H and tritiogenic ^{3}He$_{tri}$ (^{3}He produced by the decay of ^{3}H) as follows (Torgersen et al. 1979):

$$\tau_{3He} = \frac{1}{\lambda} \cdot \ln\left(1 + \frac{^3\mathrm{He}_{tri}}{^3\mathrm{H}}\right) \quad (1)$$

^{3}H concentrations are usually given in tritium units (TU; 1 TU corresponds to a ^{3}H:^{1}H ratio of 10^{-18}) and ^{3}He concentrations in cm^3 at standard temperature and pressure (STP) g^{-1}.One tritium unit of ^{3}H is equivalent to 2.49×10^{-15} cm^3 STP g^{-1} of ^{3}He$_{tri}$. Whereas the ^{3}H concentration can directly be measured, the tritiogenic ^{3}He constitutes only a fraction of the measured total ^{3}He. The major ^{3}He component in lakes is usually derived from equilibration with the atmosphere. Other components can originate from dissolution of air bubbles (excess air) and the He degassing from the Earth's crust or mantle (Kipfer et al. 2002). Atmospheric equilibrium concentrations were calculated from the solubilities of Weiss (1971), as outlined by Aeschbach-Hertig et al. (1999), using the measured water temperature and conductivity and an atmospheric pressure of 983.9 mbar, corresponding to the long-term mean pressure at the meteorological station of Lugano reduced to the altitude of the lake surface of 271 m above sea level.

Significant ^{4}He supersaturations in the deep water indicate the presence of an He flux from the sediment. We refer to this component as terrigenic He, comprising the potential contribution of He from the Earth's crust and the Earth's mantle. The separation of the He components is simplified by the fact that the measured Ne concentrations lie close to atmospheric solubility equilibrium. Thus, a correction for excess air based on the measured Ne is not necessary. ^{3}He$_{tri}$ was calculated from the following equation (Kipfer et al. 2002):

$$^3\mathrm{He}_{tri} = {}^4\mathrm{He}_m \cdot (R_m - R_{ter}) - {}^4\mathrm{He}_{eq} \cdot (R_{eq} - R_{ter}) \quad (2)$$

where ^{4}He$_m$ is the measured concentration of ^{4}He, ^{4}He$_{eq}$ is the calculated equilibrium concentration of ^{4}He, R_m is the measured ^{3}He:^{4}He ratio, R_{eq} is the ^{3}He:^{4}He ratio at solubility equilibrium ($R_{eq} \approx 1.36 \times 10^{-6}$ [Benson and Krause 1980]; significantly lower than the atmospheric ^{3}He:^{4}He ratio $R_a = 1.384 \times 10^{-6}$ [Clarke et al. 1976]), and R_{ter} is the terrigenic ^{3}He:^{4}He ratio. Note that the differences are taken between isotope ratios rather than between ^{3}He concentrations, because the ratios are usually measured with higher precision. The analytical precision of the ^{3}He:^{4}He ratio measurement of about 0.4% essentially determines the precision of the apparent ^{3}H-^{3}He age.

In order to evaluate Eq. 2, a value for R_{ter} is needed. Usually, terrigenic He is assumed to be radiogenic (derived from U and Th decay chains), with a typical ^{3}He:^{4}He ratio of 2×10^{-8} (Mamyrin and Tolstikhin 1984). However, a contribution of mantle He cannot a priori be excluded, although so far it has only been found in lakes in volcanic areas (e.g., Kipfer et al. 2002). ^{3}He:^{4}He ratios found in volcanic lakes range up to about 10^{-5}, a value typical for mid ocean ridge basalts. Since the observed ^{3}He:^{4}He ratios in the deep water of Lake Lugano reach unusually high values of up to 4.6×10^{-6}, the possibility of a presence of mantle He has to be considered.

The best way to constrain the value of R_{ter} is to derive it from samples that contain large concentrations of terrigenic He from the local or regional source. For example, hydrothermal water entering the northern basin of Lake Baikal was found to have a similar He isotopic composition as nearby hot springs on land (Kipfer et al. 1996). However, in the case of Lake Lugano, no such samples are available. An indication of the typical terrigenic ^{3}He:^{4}He ratio in the region can be found in the overview of He isotopes in fluids of the Alpine region described by Marty et al. (1992). This study shows that mantle ^{3}He is virtually absent in the main Alpine block. Gas bubbles (mainly CO_2) emanating from nearby Lago Maggiore were found to contain terrigenic He with a ^{3}He:^{4}He ratio of less than 0.1 R_a. Therefore, R_{ter} is likely to be much smaller than R_m and R_{eq}, rendering the correction for terrigenic ^{3}He small. In the absence of a better estimate, the typical radiogenic ^{3}He:^{4}He ratio of 2×10^{-8} was used in Eq. 2 for R_{ter}. If, instead, a value of 0.1 R_a would be assumed, the resulting apparent ^{3}H-^{3}He ages would be reduced by less than 0.1 yr, a value that is smaller than the typical age uncertainty of 0.3 yr.

The calculation of apparent SF_6 ages is based on the history of atmospheric SF_6 concentrations, which have increased steadily since about 1970. Figure 2 shows the time series of the SF_6 mixing ratio in remote northern hemisphere air given in IAEA (2006), which was used in this study. However, as shown by Ho and Schlosser (2000), the local mixing ratio of SF_6 near source areas can significantly exceed the background values. We are not

aware of data on the SF_6 mixing ratios in the region of Lake Lugano. The urban agglomeration of Lugano, with less than 100,000 inhabitants and a service-oriented economy, is unlikely to be a major source. However, the large industrial center of Milano (Italy) lies only about 70 km to the south. A certain atmospheric SF_6 excess can therefore not be excluded.

The atmospheric history of SF_6 is imprinted in surface waters by gas exchange. Because SF_6 behaves quasi-conservatively in water, its concentration can be interpreted in terms of the water residence time with respect to gas exchange at the surface. To this end, the atmospheric mixing ratio of SF_6 that corresponds to solubility equilibrium with each observed dissolved concentration was calculated using the solubility data of Bullister et al. (2002), the measured water temperature and conductivity, and an atmospheric pressure of 983.9 mbar. This mixing ratio was then compared with the historical increase in the atmosphere to obtain the time of the last contact of the water with the atmosphere. The apparent SF_6 age is defined as the difference between that time and the time of sampling.

Results

Temperature and conductivity The profiles of water temperature and electrical conductivity that were measured during the tracer sampling campaigns are shown in Fig. 3. The temperature profiles exhibit large seasonal temperature fluctuations in the upper 30 m of the water column (Fig. 3A). The relatively mild climate is reflected by the surface-water temperatures (minimum 6°C in March 1996). Below 100 m in depth, some profiles show an inversion (i.e., an increase of temperature with depth). Another notable feature of the temperature profiles is the continuous increase of the deep-water temperature over time. The profiles of May 1990 and May 2001 look similar in the deep water, but the latter is shifted by about 0.4°C toward higher temperatures.

The electrical conductivity (normalized to 20°C) varies seasonally in the shallow water but is almost constant over time in the deep water (Fig. 3B). The shape of all conductivity profiles in the deep water is very similar. The steady increase of conductivity (i.e., of the concentration of dissolved ions) with depth contributes decisively to the density stratification of the water column of the deep water, overcompensating for the occasional inverse temperature stratification. The strongest conductivity gradients are located between about 50 and 80 m in depth. In the lowermost 100 m of the water column, the increase of conductivity is only about 5 μS cm $^{-1}$.

The main feature of the dissolved oxygen profiles (not shown) is that the oxygen concentration drops to zero at a depth of approximately 80 m. In spring, the oxygenated depth tends to be slightly higher, but it never becomes significantly deeper than 100 m. The permanent anoxia of the deep water below 100 m is a characteristic feature of the Northern Basin of Lake Lugano that has been discussed in many previous studies (e.g., LSA 1981 2000; Barbieri and Mosello 1992; Barbieri and Simona 2001).

Transient tracers All tracer results are summarized in Tables 1 (^{3}H and He data) and 2 (CFC and SF_6 data). The ^{3}H concentrations in the deep water of Lake Lugano steadily decreased over the observed period from ~50 TU in 1990 to ~20 TU in 2001 (Fig. 4A). All ^{3}H profiles show a concentration increase between about 40 and 120 m in depth and rather constant concentrations at greater depth. The high regularity of the ^{3}H profiles made it possible to estimate some missing ^{3}H values from interpolation in space and time (*see Table 1*). Interpolated ^{3}H values are not shown in Fig. 4A, but the respective ^{3}H-^{3}He ages appear reasonably reliable and are used in the following. The general features of the ^{3}H distribution are readily understood as the result of the time dependence of the ^{3}H input from precipitation (Fig. 2) and a relatively slow exchange of the deep water. The high ^{3}H concentrations in the deep water are a relict of the high ^{3}H input in the 1960s and 1970s. The lower concentrations in the surface water reflect the lower ^{3}H concentrations in contemporary precipitation.

The He concentrations also reflect the vertically layered structure of Lake Lugano. All ^{4}He profiles look very similar, exhibiting a strong increase from the surface down to a depth of about 120 m and a very weak increase at greater depth (Fig. 4B). There is a weak but significant temporal trend of increasing concentrations in the deep water. Concentrations in the surface mixed layer are close to equilibrium with the atmosphere at the surface water temperature. Concentrations in the deep water correspond to supersaturations of up to approximately 15% relative to the corresponding equilibrium concentration (about 4.6×10^{-8} cm^3 STP g^{-1}). This supersaturation of He in the deep water is indicative of the presence of terrigenic He.

The ^{3}He profiles have similar general features as the ^{4}He profiles, with concentrations near solubility equilibrium in the surface mixed layer and an enrichment in the deep water (Fig. 4C). However, the depth range with a strong gradient of the ^{3}He concentration profile extends down to a greater depth (about 180 m). Moreover, the supersaturation in the deepest part of the water column is much larger than for ^{4}He (up to 280%). In contrast to the weak increasing time trend of the ^{4}He concentrations, the ^{3}He concentrations slightly decreased after having reached a maximum in 1992, and the decrease has accelerated since then.

The calculated ^{3}He : ^{4}He ratio of the excess He (He above solubility equilibrium) in the deep-water samples decreased continuously from almost 4×10^{-5} in 1990 to less than 2×10^{-5} in 2001. These values are higher than any ratios observed for terrigenic He components in lakes, implying that tritiogenic ^{3}He is the major excess ^{3}He component. The differences between the ^{3}He and ^{4}He profiles and the decrease of the isotope ratio with time show that the He excess in the deep water has at least two sources. While terrigenic ^{4}He and the corresponding small ^{3}He component are still accumulating, the concentration of tritiogenic ^{3}He is decreasing along with the ^{3}H content.

The SF_6 profile from May 2001 shows the expected decrease with depth (Fig. 5). The SF_6 concentration of the surface sample is 16% higher than the atmospheric

Table 1. Results of ^3H and He isotope analyses and apparent ^3H ^3He ages.

Depth (m)	^3H (TU)	$^4He \times 10^8$ (cm^3 STP g $^{-1}$)	$^3He : ^4He \times 10^6$	Age (yr)
		Sampling date: 16 May 1990*		
0	*32.14±2.00*†	4.392±0.057	1.367±0.007	*0.14±0.18*†
20	35.49±1.40	4.608±0.060	1.531±0.008	1.64±0.19
50	36.14±1.06	4.716±0.062	1.981±0.009	5.24±0.23
70	*40.60±2.00*†	4.711±0.061	2.615±0.011	*8.35±0.38*†
90	42.96±1.46	4.822±0.065	3.216±0.014	11.07±0.34
110	44.51±1.29	5.021±0.066	3.587±0.015	12.85±0.33
120	46.22±1.23	4.859±0.063	3.792±0.013	12.82±0.31
140	46.19±1.01	4.798±0.063	4.003±0.019	13.41±0.28
150	47.00±1.48	4.941±0.064	4.129±0.017	14.08±0.36
165	47.46±1.17	4.851±0.064	4.266±0.011	14.19±0.31
180	46.90±1.33	5.203±0.069	4.328±0.016	15.50±0.35
200	*49.12±2.00*†	5.127±0.067	4.424±0.014	*15.13±0.46*†
210	*49.39±2.00*†	5.036±0.066	4.501±0.017	*15.06±0.45*†
235	47.73±1.47	5.026±0.066	4.540±0.018	15.51±0.37
250	*49.90±2.00*†	5.080±0.066	4.584±0.018	*15.34±0.45*†
265	51.13±1.33	5.073±0.067	4.448±0.016	14.66±0.32
275	49.64±1.38	5.237±0.068	4.549±0.021	15.71±0.35
285	49.18±1.26	5.199±0.068	4.599±0.019	15.87±0.33
		Sampling date: 01 Dec 1992		
0	24.21±0.63	4.510±0.028	1.392±0.008	0.43±0.15
25	28.88±0.67	4.668±0.028	1.608±0.007	2.95±0.13
50	30.08±0.64	4.762±0.029	1.956±0.010	6.08±0.17
70	32.38±0.69	4.814±0.029	2.374±0.011	8.80±0.19
90	35.28±0.71	4.964±0.030	3.122±0.014	12.77±0.22
110	39.03±0.75	4.974±0.032	3.639±0.020	14.16±0.23
130	39.43±0.80	Sample lost	Sample lost	Sample lost
150	40.74±0.76	5.100±0.031	4.190±0.019	16.21±0.23
170	40.51±0.75	5.107±0.031	4.340±0.019	16.82±0.23
190	41.56±0.77	5.139±0.031	4.419±0.019	16.91±0.23
210	40.31±0.71	5.145±0.031	4.505±0.019	17.56±0.23
233	42.23±0.86	5.183±0.032	4.549±0.020	17.30±0.25
258	42.29±0.77	5.174±0.032	4.514±0.016	17.14±0.23
283	42.03±0.76	5.234±0.032	4.490±0.019	17.30±0.23
		Sampling date: 10 Oct 1993		
0	21.07±1.32	4.448±0.017	1.384±0.008	0.45±0.14
50	28.59±0.70	4.710±0.018	1.904±0.010	5.74±0.16
100	35.27±0.66	4.999±0.019	3.254±0.013	13.51±0.20
125	36.85±1.95	5.061±0.019	3.726±0.016	15.36±0.55
150	*37.36±2.00*†	5.158±0.019	4.083±0.014	*16.92±0.59*†
175	*37.46±2.00*†	5.129±0.019	4.278±0.018	*17.53±0.60*†
200	37.94±0.74	5.170±0.019	4.413±0.017	17.99±0.24
225	38.89±1.47	5.162±0.019	4.455±0.016	17.84±0.43
250	41.37±1.43	5.201±0.020	4.479±0.018	17.35±0.39
284	38.65±0.75	5.128±0.046‡	4.534±0.049‡	18.08±0.24
		Sampling date: 06 Sep 1994		
0	*21.27±2.00*†	4.374±0.031	1.363±0.008	*0.36±0.19*†
100	*32.89±2.00*†	5.159±0.037	3.253±0.017	*14.68±0.62*†
150	*35.62±2.00*†	5.250±0.037	4.012±0.018	*17.45±0.64*†
189	*36.68±2.00*†	5.200±0.037	4.333±0.021	*18.18±0.64*†
214	*36.63±2.00*†	5.263±0.037	4.299±0.019	*18.27±0.64*†
248	*38.34±2.00*†	5.251±0.037	4.380±0.018	*18.00±0.60*†
		Sampling date: 06 Mar 1996		
2	21.62±0.80	4.687±0.012	1.552±0.007	3.10±0.15
50	22.80±0.56	4.731±0.019	1.615±0.006	3.89±0.14
100	28.84±0.89	5.078±0.008	3.197±0.009	15.48±0.32
125	32.22±0.92	5.200±0.009	3.605±0.010	16.68±0.31
150	32.64±0.91	5.237±0.009	3.860±0.009	17.76±0.32
175	35.88±1.66	5.253±0.009	4.085±0.011	17.67±0.52

Table 1. Continued.

Depth (m)	^{3}H (TU)	^{4}He×10^8 (cm^3 STP g $^{-1}$)	^{3}He : ^{4}He×10^6	Age (yr)
200	34.38±0.95	5.264±0.009	4.193±0.010	18.60±0.32
225	33.08±0.90	5.266±0.009	4.220±0.009	19.16±0.32
250	33.43±0.61	5.289±0.020	4.221±0.013	19.11±0.23
280	34.18±1.02	5.304±0.009	4.239±0.010	18.96±0.35
		Sampling date: 19 Sep 1996		
50	22.38±0.65	4.744±0.008	1.744±0.006	5.52±0.16
100	25.83±0.79	5.098±0.008	3.009±0.008	15.65±0.32
125	*27.96±2.00*†	5.186±0.009	3.420±0.009	*17.31±0.79*†
150	30.09±0.74	5.215±0.009	3.737±0.009	18.08±0.28
175	30.02±0.71	5.250±0.009	3.850±0.010	18.72±0.28
200	31.92±0.88	5.281±0.009	3.998±0.011	18.73±0.32
225	32.89±0.84	5.276±0.009	4.085±0.010	18.72±0.30
250	31.76±0.72	5.295±0.009	4.107±0.010	19.28±0.27
280	31.40±0.78	5.302±0.009	4.151±0.009	19.61±0.30
		Sampling date: 03 May 2001		
50	14.55±2.25	4.876±0.013	1.717±0.009	8.18±1.02
125	18.85±0.41	5.121±0.016	2.905±0.010	18.53±0.27
200	21.04±0.47	5.312±0.014	3.582±0.011	21.95±0.29
283	21.17±0.34	5.405±0.016	3.683±0.011	22.72±0.22

* The major part of the profile from May 1990 was already presented in Wuest et al. (1992). TU, tritium units. STP, standard temperature and pressure, O°C, 1 atm.

† ^{3}H values in italics are interpolated from samples above and below or (in the case of the 1994 profile) from neighboring profiles in time. ^{3}He ^{3}He ages in italics are based on the interpolated ^{3}H values with the assigned error of ±2 TU.

‡ He data for this sample corrected for air contamination based on Ne (9.0% Ne excess).

equilibrium concentration calculated from the 2001 remote air SF_6 mixing ratio of 5.0 ppt and the measured water temperature of 12.1°C. This supersaturation is probably due to the strong temperature dependency of the SF_6 solubility and the enhanced atmospheric SF_6 mixing ratios. There may be a time lag between surface-water warming in spring and the corresponding SF_6 outgassing. The measured SF_6 concentration would be in equilibrium with 5.0 ppt SF_6 in air at a water temperature of 8.6°C. In addition, as mentioned above, the proximity of the city of Milano may lead to elevated SF_6 concentrations in the local air. This effect would imply a bias in the apparent SF_6 ages. If, for example, the local atmospheric mixing ratios were elevated by 10% relative to clean-air values, the SF_6 ages would be too young by 1 to 2 yr.

Discussion

Temperature, conductivity, and stability Characteristic features of the CTD data in the deep water are the occurrence of inverse temperature stratification, the continuous temperature increase with time, the persistent gradient of conductivity, and the permanent absence of oxygen. These observations indicate that the lake is meromictic (i.e., seasonal convection in winter/spring does not reach the lake bottom). The water density and, hence, the stratification are determined by temperature and salinity. Salinity was calculated from the measured conductivity using a conversion factor of 0.89×10^{-3} ‰ (μS cm $^{-1}$) $^{-1}$ derived by Wüest et al. (1992) from the measured ion composition of Lake Lugano, which is dominated by calcium and bicarbonate.

For the analysis of the vertical stratification, we calculate the local stability or Brunt Vaisälä frequency,

$$N^2 = -\frac{g}{\rho}\frac{d\rho}{dz} = g\left(\alpha\frac{dT}{dz} - \beta\frac{dS}{dz}\right) \equiv N_T^2 + N_S^2 \quad (3)$$

where α is the coefficient of thermal expansion, β is the coefficient of haline contraction, the z coordinate is positive upward, and the correction for the effect of adiabatic compression is neglected (the difference between in situ and potential temperature is only about 0.005°C at the lake bottom). In order to elucidate the origin of the density stratification, the total stability N^2 is separated into the two contributions of temperature ($N_T^2 = g\alpha dT/dz$) and salinity ($N_S^2 = -g\beta dS/dz$). Note that N^2 is not affected by possible calibration offsets of T and S because it only depends on their gradients.

Figure 6 shows as an example the profile of N^2 from December 1992, with the individual terms in the deep water shown in the inset. The stability profiles calculated for the other samplings are very similar, in particular in the deep water. Differences only occur in the upper ~50 m of the water column, where the stability is dominated by temperature and reaches its maximum in the thermocline. In the deep water below about 80 m in depth, the influence of temperature on stability is neutral or even negative. The stratification is nevertheless always stable because the persistent gradient of salinity entirely dominates the stability. The constancy of the conductivity gradients over time implies constant density stratification of the deep water. The stability reaches a minimum of $\sim 3 \times 10^{-7}$ s $^{-2}$ around 240 m in depth. The bottom layer has a somewhat higher stability as

Table 2. Results of chlorofluorocarbons (CFC) and sulfur hexafluoride (SF_6) analyses and apparent SF_6 ages.

Depth (m)	CFC 11 (pmol kg $^{-1}$)	CFC 12 (pmol kg $^{-1}$)	SF_6 (fmol kg $^{-1}$)	SF_6 age (yr)
		Sampling date: 06 Mar 1996		
2	7.81±0.14	7.01±0.11		
50	8.10±0.15	6.66±0.10		
100	3.24±0.06*	7.58±0.11		
125	1.78±0.03*	7.99±0.12		
150	1.27±0.02*	7.17±0.11		
175	0.83±0.01*	7.33±0.11		
200	0.85±0.02*	6.97±0.10		
225	0.90±0.02*	7.36±0.11		
250	0.54±0.01*	7.00±0.10		
280	1.12±0.02*	7.70±0.12		
		Sampling date: 19 Sep 1996		
0	4.05±0.07	4.33±0.07		
50	7.13±0.13	6.03±0.09		
100	3.74±0.07*	6.79±0.10		
125	1.91±0.03*	7.15±0.11		
150	1.12±0.02*	7.10±0.11		
175	0.94±0.02*	6.94±0.10		
200	0.82±0.01*	7.17±0.11		
225	0.72±0.01*	6.92±0.10		
250	0.78±0.01*	6.93±0.10		
280	0.75±0.01*	6.69±0.10		
		Sampling date: 03 May 2001		
0		4.19±0.21	2.02±0.10	<0
25		5.24±0.26	1.73±0.09	4.5±0.7
50		5.64±0.28	1.84±0.09	4.0±0.8
75		6.11±0.31	1.66±0.08	5.5±0.7
100		6.52±0.33	1.26±0.06	9.3±0.6
125		6.39±0.32	1.33±0.07	8.6±0.6
150		7.18±0.36	1.16±0.06	10.3±0.6
175		6.90±0.34	1.23±0.06	9.6±0.6
200		7.09±0.35	1.08±0.05	11.2±0.6
225		6.73±0.34	1.14±0.06	10.6±0.6
250		7.14±0.36	0.99±0.05	12.3±0.6
283		6.78±0.34	0.94±0.05	12.8±0.5

* CFC 11 concentrations from the anoxic deep water (≥100 m in depth) were corrected for degradation during storage in the copper tubes using the rate determined by Hofer and Imboden (1998).

the result of an increased gradient of salinity. Because in some profiles temperature and salinity have opposing effects on the stratification of the water column, so-called double diffusion (mixing due to differential diffusion of heat and dissolved ions: e.g., Imboden and Wüest 1995) could occur in principle. However, Wüest et al. (1992) found that double diffusion is of minor importance in Lake Lugano.

The increase of the deep-water temperature by about 0.4°C during the period of tracer measurements (1990 2001; Fig. 3A) is corroborated by an analysis of the temperature data of the LSA (LSA 1998). Figure 7 shows volume-weighted mean temperatures below different depths (0, 50, 100, 150, and 200 m) calculated from these data for the 12-yr period from 1987 through 1998. This data series documents a quite uniform warming during the 1990s. Linear fits to the data from 1990 through 1998 yield warming rates of 0.05°C yr $^{-1}$ for the entire water mass below 50 m in depth and rates of around 0.03°C yr $^{-1}$ for the water bodies below 100, 150, and 200 m in depth. Figure 7 also shows that a strong inverse temperature stratification was present in the late 1980s, until it was reduced by a mixing event. After that event, the temperature gradients between 50 and 150 m in depth were weak and of alternating sign, while below 150 m in depth the inverse stratification persisted. In 1994 a regular stratification (T decreasing with depth) began to build up in the entire water column, and this stratification continuously strengthened. As is evident in Fig. 3A, the temperature gradient in the deep water has again changed sign by 2001. Such observations show that although deep-reaching mixing events are rare, the deep water is not entirely isolated. Changing conditions at the surface have an effect on the deep water, but the predominant characteristic of the deep-water evolution is a slow warming.

Several processes may affect the heat balance of the deep water: (1) geothermal heating, (2) density currents, (3) deep-reaching convection, and (4) vertical turbulent diffusion. The heating of the deep water by the geothermal heat flow can be estimated quite accurately. Heat flow measurements in the sediments of Lake Lugano by Finckh

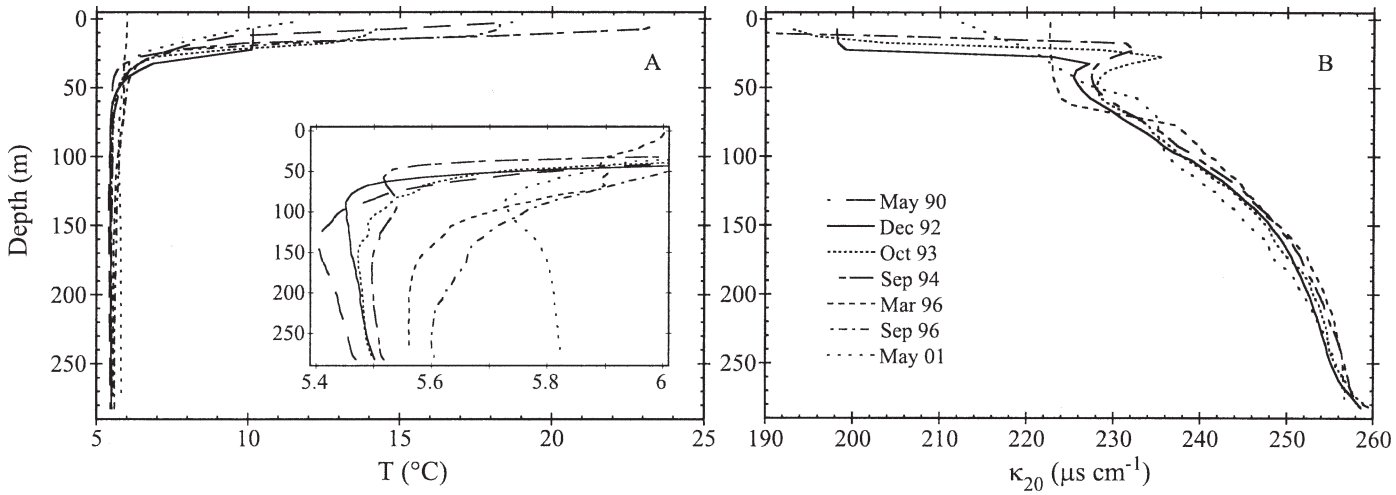

Fig. 3. CTD profiles taken during the tracer sampling campaigns (including data from May 1990 of Wüest et al. [1992]). (A) Temperature. The inset shows an enlargement of the deep water temperatures. (B) Electrical conductivity normalized to 20°C (κ_{20}). Month and year of the sampling campaigns are given in the legend in panel B. The conductivity profiles from May 1990 and September 1996 were omitted because of missing calibration functions. The uncalibrated profiles are offset from the other profiles by 10 to 20 μS cm ^{1}, but agree in their shape.

(1981) yielded values of 97 $\pm$ 10 mW m ^{2}. If the water mass below 150 m in depth (volume 1.4 $\times$ 10^{9} m^{3}, area 1.6 $\times$ 10^{7} m^{2}) was affected only by this heat flux, it should warm by about 0.008°C yr ^{1}. This purely geothermal warming trend is shown in Figure 7 for comparison. The actual overall warming trend below 150 m in depth between 1987 and 1998 was stronger (0.02°C yr ^{1}), and the thermal history of the deep water was much more variable than expected from geothermal heating only. Thus, other heat transport mechanisms must play a major role.

Such a mechanism could involve advective transport of water masses to greater depth (i.e., density currents). Since the Northern Basin of Lake Lugano has a simple shape without sills, topography-driven exchange currents, as postulated for Lake Lucerne (Aeschbach-Hertig et al. 1996) or Lake Baikal (Peeters et al. 1997), are not an option. Formation of significant amounts of cold water in shallow areas near the shore is also unlikely because of the steep topography of the basin. Turbidity currents during floods of the tributary rivers are a plausible mechanism of deep-water exchange. Such currents could produce both cooling and warming, depending on the temperature of the river and the entrained surface water. Yet, given the rather low inflow to the lake, the overall effect of river-induced density currents is expected to be minor. Lavelli et al. (2002) modeled three events in 1994, 1999, and 2000, in which the turbidity current induced by flood waters of the

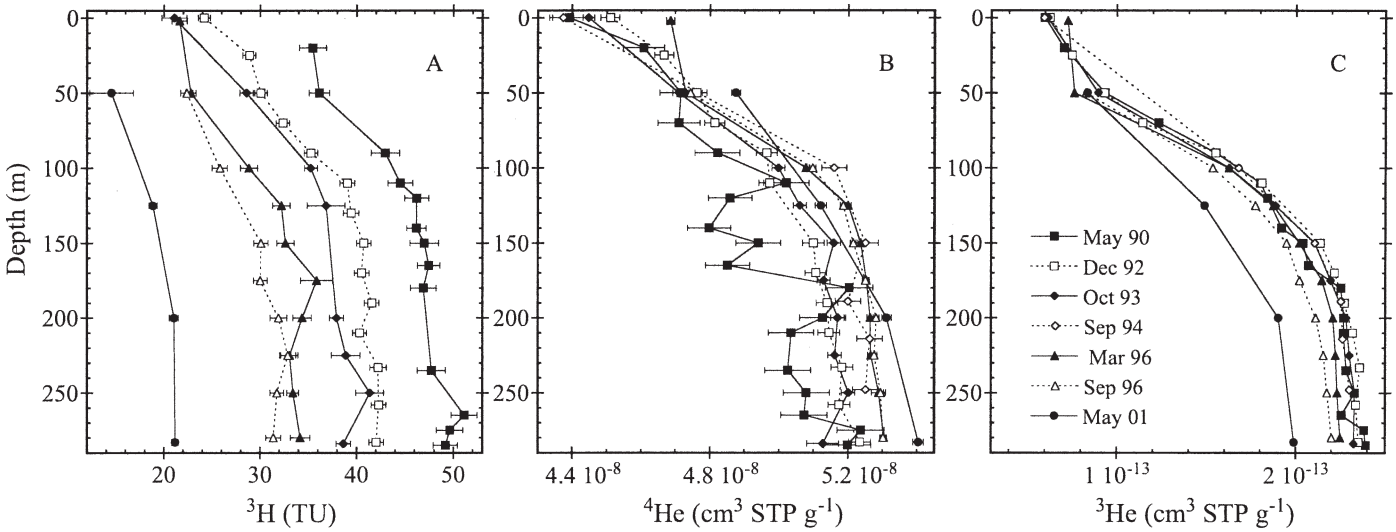

Fig. 4. Depth profiles of the transient tracers (A) ^{3}H, (B) ^{4}He, and (C) ^{3}He (including data from May 1990 in part already presented in Wüest et al. [1992]). Month and year of the sampling campaigns are given in the legend in panel C. Uncertainties for ^{3}He are of approximately the same size as the symbols. See Table 1 for further details.

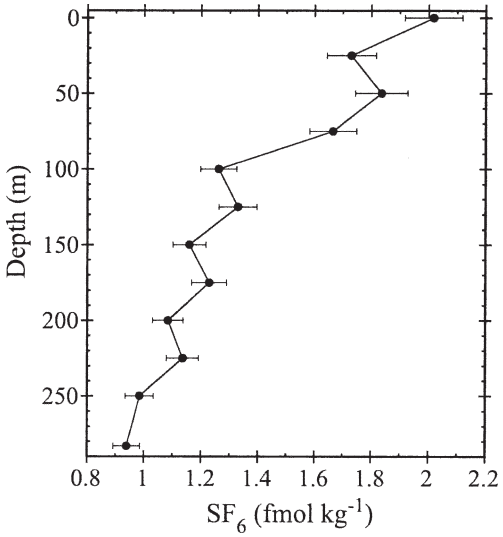

Fig. 5. Depth profile of SF_6 concentrations from the sampling on 03 May 2001.

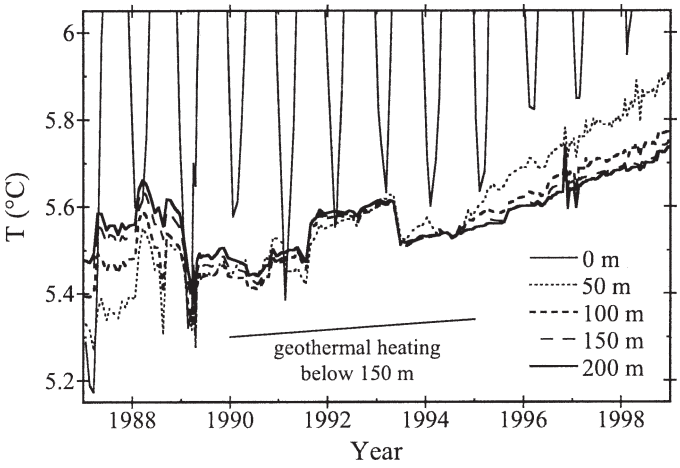

Fig. 7. Temporal evolution of the heat content of the deep water of Lake Lugano between 1987 and 1998, based on the regular LSA CTD profiles (e.g., LSA 1998). Volume weighted mean temperatures below the specified depths are shown.

main tributary Cassarate reached the deepest part of the basin. Even the exceptional flood of September 1994 (1 week after our sampling) did not have a strong and long-lasting effect on the structure of the water column (*see Figs. 3*, *7*).

Convective mixing of the entire water column is only possible if the surface cools to a lower temperature than the deep water, and convective mixing should therefore lead to cooling of the deep water. In Fig. 7, such events are indicated if the minima of the line for the mean temperature of the entire lake (0 m) fall below the deep-water temperatures, which is only rarely the case. Of these few events, apparently only the one in spring 1989 had a significant cooling effect on the entire deep water. This behavior is quite different from that of similar lakes on the northern flank of the Alps, where Livingstone (1997) observed a "sawtooth" structure of gradual warming punctuated by abrupt cooling by turnovers occurring in cold winters. In contrast to the effects on these lakes, the cold winters of 1987 and 1991 had only weak effects on Lake Lugano.

The fact that low surface-water temperatures on their own do not guarantee deep mixing in Lake Lugano can be understood by comparing the density effects of temperature and salinity. The conductivity difference of about 30 μS cm ^{1} between shallow and deep water (*see Fig. 3B*, e.g., March 1996 profile between 50 and 200 m) corresponds to a density difference of 0.023 kg m ^{3}. This is equivalent to the density difference between pure water of 4.0°C and 5.7°C. Since the deep-water temperature in 1990 was below 5.5°C (Figs. 3A, 7), even cooling of the shallow water to the temperature of maximum density (4°C) could not force convective mixing. However, at some time in the late 1990s the deep-water temperature rose to above 5.7°C, thus passing a threshold and enabling convective mixing if the surface water cools sufficiently.

Yet during our observation period, a turnover of the water column was prevented by mild climatic conditions in concert with the chemically induced density stratification. The recent development of the temperature regime and mixing dynamics of Lake Lugano may be seen as an example of how changing climatic conditions affect a lake system. Based on the data of Begert et al. (2005), the 1990s were the warmest decade in Lugano since the beginning of the records in 1864. This holds true in particular for the winter and spring temperatures. The warming trend during our observation period of 1990 2001 was 0.03°C yr ^{1} for the annual mean air temperatures and 0.09°C yr ^{1} for the winter months (Dec/Jan/Feb).

Although the air and the deep water warmed at about the same rate during this period, the situation changed fundamentally when the deep-water temperature passed the above-mentioned threshold. The increasing air temperatures still kept the stratification stable, but the stage was set

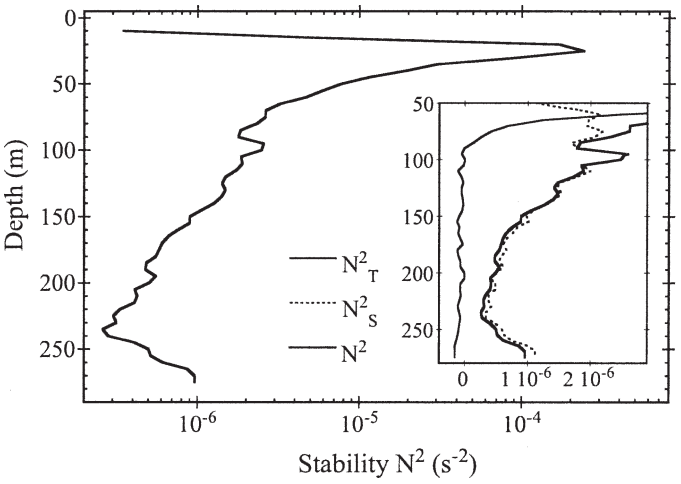

Fig. 6. Profiles of the Brunt Vaisälä stability frequency N^2 and its components due to temperature (N_T^2) and salinity (N_S^2) gradients, shown as an example for the data from 01 December 1992. The main figure shows N^2 on a logarithmic scale. The inset shows N_T^2 and N_S^2 below 50 m in depth on a linear scale.

such that sooner or later a cold winter, possibly supported by strong winds (an increasing trend is present in the meteorological data of Lugano for the period from 1971 to 2000), could induce deep-reaching circulation. In fact, the complete turnover that occurred in Lake Lugano in early 2005 has been ascribed to an unusually cold and windy winter (SPAAS 2005).

Finally, turbulent diffusion is a permanently active mechanism of vertical heat transport. It can have both a cooling and a warming effect on the deep water, depending on the sign of the temperature gradient (Fig. 7). In the period between 1987 and 1990, when the inverse stratification was most pronounced, the time trend of temperature below 150 m in depth was negative (0.03°C yr ^{1}). During times of small deep-water temperature gradients (e.g., 1990 1993), turbulent diffusion cannot have a strong effect on temperature, and the warming is comparable to the geothermal trend. Between 1994 and 1998, a strong regular temperature gradient developed, and the warming trend for the water mass below 150 m in depth was as large as 0.04°C yr ^{1}, about five times stronger than expected from geothermal heating alone. Assuming that only turbulent diffusion and geothermal heating contributed to this warming trend, it can be used to derive a rough estimate of the vertical turbulent diffusivity in the hypolimnion by the budget-gradient method.

In this general method, originally introduced by Jassby and Powell (1975), the rate of change of the heat content Q_z below a certain level z (the vertical coordinate z is directed upward) is set equal to the turbulent diffusive downward heat flux F_{diff} across the corresponding cross-sectional area A_z plus the geothermal heat flux F_{geo}. According to Fick's law, the diffusive flux depends on the vertical temperature gradient, and the balance equation can be written as

$$\frac{dQ_z}{dt} = A_z \cdot (F_{geo} + F_{diff}) = A_z \cdot \left(F_{geo} + K_z c \rho \frac{dT}{dz} \right) \quad (4)$$

where c is the heat capacity of water and ρ is water density. Since the warming rate between 1994 and 1998 was about five times stronger than expected from geothermal heating alone, the diffusive downward flux F_{diff} must be about four times as large as the geothermal flux, or about 0.4 W m ^{2}. The typical temperature gradient at 150 m in depth is roughly estimated from the profiles of 1994 and 1996 to be 0.001°C m ^{1}. From Eq. 4 we then obtain an estimate of K_z at 150 m in depth of 10 ^{4} m^2 s ^{1}.

Using similar arguments, Livingstone (1997) showed that K_z values on the order of 10 ^{4} m^2 s ^{1} are consistent with similar deep-water warming trends observed in other perialpine lakes. For the deep water of Lake Lugano, Wüest et al. (1992) derived an increase of K_z from about 3 $\times$ 10 ^{5} m^2 s ^{1} at 150 m in depth to 1 $\times$ 10 ^{4} m^2 s ^{1} at the lake bottom from a balance between diffusive cooling and geothermal heating based on the temperature profile from May 1990. Aeschbach-Hertig (1994) obtained a K_z value of 2 $\times$ 10 ^{5} m^2 s ^{1} at 150 m and a maximum of 7 $\times$ 10 ^{5} m^2 s ^{1} at 200 m in depth from a ^{3}He balance for the years 1990 to 1992. Our K_z estimate of 10 ^{4} m^2 s ^{1} at 150 m in depth is, thus, rather high, but acceptable in view of the large uncertainties involved, in particular for the value of the temperature gradient.

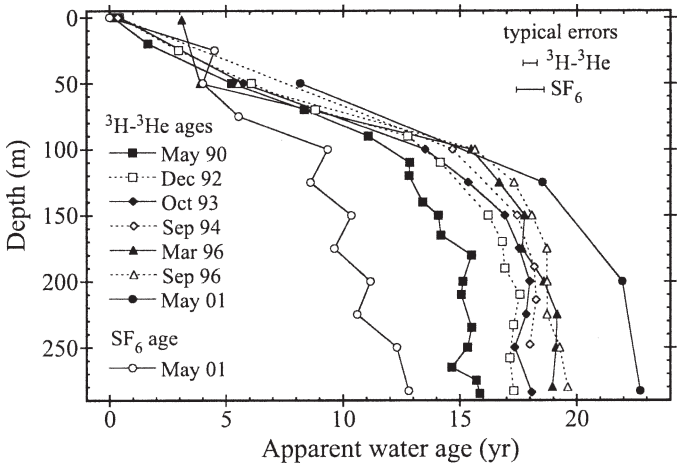

Fig. 8. Profiles of apparent tracer ages. ^{3}H ^{3}He ages for the seven sampling campaigns between 1990 and 2001 are shown together with the SF_6 age profile from 2001.

Equation 4 can be applied to any interval between temperature profiles and evaluated at any depth level, if changes in heat content and vertical temperature gradients can be determined with sufficient precision and if turbulent diffusion can explain the observed evolution. In the case of Lake Lugano, the latter condition is often not fulfilled, because Q_z generally increases, whereas the vertical temperature gradient, and thus the direction of the diffusive flux, often change sign. The only interval between two tracer samplings during which the temperature gradient probably remained always positive is between March and September 1996. A calculation of K_z from these temperature profiles is discussed below along with results obtained from the ^{3}He profiles.

Apparent tracer ages Profiles of the calculated apparent ages for ^{3}H-^{3}He and SF_6 are shown in Fig. 8. All ^{3}H-^{3}He age profiles measured between 1990 and 2001 have a similar shape, characterized by a strong and nearly linear increase with depth in the shallow water and only a slight further increase in the deep water below 100 m in depth. The apparent ^{3}H-^{3}He ages in the deep water increased continuously with time over the studied period, with maximum ages at the bottom of 16 yr in 1990 and 23 yr in 2001. While the increase of apparent age indicates little renewal of the deep water, the fact that the apparent age increased only by roughly 7 yr in 11 yr of real time also shows that the deep water did not evolve as a closed system. In agreement with conclusions drawn from the temperature data, the evolution of the ^{3}H-^{3}He age shows that some limited exchange of the deep water must have taken place.

The SF_6 age profile from 2001 exhibits a similar shape to the ^{3}H-^{3}He age profiles, but with considerably younger ages, reaching a maximum of 12.8 yr at the lake bottom. In

the deep water the difference between SF_6 ages and the corresponding ^3H-^3He ages amounts to about 10 yr. Even if it is considered that the apparent SF_6 ages might be 1 2 yr too young as a result of locally enhanced atmospheric SF_6 mixing ratios, a large difference between the two apparent tracer ages remains. This difference can qualitatively be explained by the different effects of mixing for the two methods. The definitions of the tracer ages assume that no mixing occurs. Since the deep water of Lake Lugano (and presumably of most meromictic lakes) experiences exchange and mixing with the shallower layers, the apparent tracer ages deviate from the true mean isolation age of the mixed water.

The nonlinearity of the apparent ^3H-^3He age with respect to the concentrations of ^3H and ^3He is obvious from the defining Eq. 1. Mixing of water with different ^3H concentrations and different ages always leads to a bias of the apparent age of the mixture toward the age of the component with the higher ^3H concentration (e.g., Jenkins and Clarke 1976; Kipfer et al. 2002; Schlosser and Winckler 2002). In the case of Lake Lugano during the study period, young surface water with low ^3H and $^3He_{tri}$ content is mixed with old deep water with high ^3H and $^3He_{tri}$ concentrations. Thus, the resulting apparent age of the mixed water tends to be too high, because the $^3He_{tri}$: ^3H ratio of the mixture remains dominated by the deep-water component.

As with the ^3H-^3He age, the SF_6 age does not behave linearly if water masses of different ages are mixed. Since the SF_6 input curve increases more strongly than linearly (positive curvature or second derivative, *see Fig. 2*), mixtures between an old and a young component always appear too young, whereas the opposite is true for CFCs (Hofer et al. 2002). Waugh et al. (2002) showed that the mean of transit time distributions for the deep water of Lake Issyk Kul was always older than the apparent SF_6 age but younger than the CFC ages. Hence, the SF_6 ages quite certainly underestimate the true mean residence time in Lake Lugano, whereas the ^3H-^3He ages most likely overestimate it, in qualitative agreement with the difference between the two tracer age profiles observed in 2001.

It is important to discuss not only the difference between the two tracer ages but also the increase of the apparent ^3H-^3He age in Lake Lugano in the context of mixing. The essential point is that the bias of the ^3H-^3He age induced by mixing is continuously changing because of the transient nature of the ^3H input. Aeschbach-Hertig (1994) used a simple mixed-reactor model to demonstrate this effect. We use an updated version of this model that describes the evolution of the concentrations of ^3H, $^3He_{tri}$, and SF_6 in a mixed box of volume V with a constant in- and outflow rate Q. The input functions for ^3H and SF_6, as shown in Fig. 2 extended back to 1900 with low constant values, were prescribed for the inflowing water. The model was numerically integrated using the software AQUASIM (Reichert 1994) starting at the year 1900, and apparent tracer ages were calculated from the modeled concentrations at all times. Figure 9 shows the evolution of the concentrations and apparent ages for the time period from 1950 to 2006, for a model run with a water exchange rate

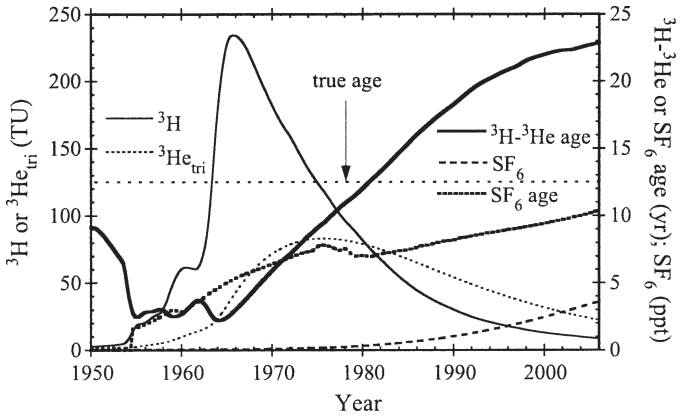

Fig. 9. Temporal evolution of the concentrations of ^3H, $^3He_{tri}$, and SF_6 as well as the apparent ^3H ^3He and SF_6 ages in a mixed reactor with a water exchange rate of 0.08 yr $^{-1}$ corresponding to a true mean residence time of 12.5 yr (compare Aeschbach Hertig [1994]). SF_6 concentrations in the water are given as equivalent atmospheric mixing ratios.

$k_{ex} = Q/V$ of 0.08 yr $^{-1}$ (the choice of this value will become clear later).

Since the exchange rate is constant, the true mean residence time of the water in the modeled box is also constant at $\tau = 1/k_{ex} = 12.5$ yr. However, most of the time the apparent tracer ages deviate strongly from this value (Fig. 9). The apparent SF_6 age increases slowly but remains more than 2 yr below the true age even by 2006. For the ^3H-^3He method, the passage of the ^3H bomb peak produces even larger and more long-lasting age distortions. The apparent ^3H-^3He age first is strongly depressed by the arrival of the bomb peak around 1960, but later rises continuously to nearly 23 yr by 2006. Interestingly, this simple model system, with constant water renewal and a true mean residence time of 12.5 yr, produces an evolution of the apparent ages that is quite comparable to that observed in the deep water of Lake Lugano. In particular, the apparent ^3H-^3He age increases by about 4 yr between 1990 and 2001 despite a constant mixing rate, and the difference between the two tracer ages is more than 12 yr in 2001. The decrease of the ^3H and $^3He_{tri}$ concentrations during the 1990s is also qualitatively correctly modeled.

It has to be stressed that this simple mixed-reactor model is not meant to quantitatively model the evolution of the deep water of Lake Lugano. The main difference is that the deep water of the lake exchanges with an extended upper water column rather than directly with contemporary surface water. As a result, the temporal variation of the input to the deep water is less extreme than in the model, and the biases of the apparent ages are probably smaller. Nevertheless, the model shows that the increase of the apparent ^3H-^3He age in the lake between 1990 and 2001 does not unequivocally imply that the true mean residence time of the deep water increased or that the mixing intensity decreased over this period.

A quantitative assessment of the influence of mixing on the apparent tracer ages would require a more sophisticated numerical model of the evolution of the various tracer

concentrations, which is beyond the scope of this study. Yet even without such a model, an analysis of the tracer concentrations rather than the apparent ages allows us to derive quantitative estimates of important process rates in Lake Lugano, such as the deep-water renewal rate or the vertical turbulent diffusivity K_z, as discussed in the following section.

^{3}H-^{3}He balance and mixing While the apparent tracer ages provide information on the deep-water residence time, it is advisable to refer to the tracer concentrations themselves for a quantitative evaluation of the exchange rates, as they are not affected by nonlinear response to mixing. The evolution of the ^{3}H and ^{3}He concentrations in Lake Lugano reflects the fact that the deep water is not isolated. In a closed system, ^{3}H concentrations would decrease according to the radioactive decay law and ^{3}He concentrations would increase correspondingly. In Lake Lugano, both ^{3}H and ^{3}He decreased during most of the study period. In the bottom water below 200 m, where the concentrations are almost constant with depth (Fig. 4), ^{3}H decreased from 50 TU in 1990 to 20 TU in 2001. An exponential fit to this decrease (not shown) yields a decay rate of 0.077 yr $^{-1}$, a value that is clearly larger than the radioactive decay rate of ^{3}H of 0.056 yr $^{-1}$. The ^{3}He concentrations initially increased slightly from 1990 to 1992 to a maximum concentration corresponding to 94 TU, but since then they have decreased almost linearly to 78 TU in 2001.

Obviously, radioactive decay is not the only process that removes ^{3}H from the deep water, and ^{3}He is removed at a higher rate than it is added by ^{3}H decay. Since both ^{3}H and ^{3}He concentrations increase with depth, turbulent diffusion results in upward fluxes of these tracers. The ^{3}H and ^{3}He data can therefore be used to estimate the vertical turbulent diffusivity K_z by the budget-gradient method. This method is usually applied to temperature data (*see Eq. 4*) but can be generalized to use the budget and vertical gradient of any conservative tracer. The change of total tracer mass below a depth z is set equal to the turbulent diffusive flux across the respective cross-sectional area A_z plus possible in situ sources. The adaptation of the method to ^{3}H and ^{3}He (the sum of which constitutes a conservative tracer) has been discussed by Aeschbach-Hertig (1994) and Kipfer et al. (2002). The budget is calculated for ^{3}He, and the source term from ^{3}H decay is calculated from the ^{3}H data. K_z is derived from the following balance equation:

$$\frac{dM_{3He,z}}{dt} = A_z \cdot K_z \frac{dC_{3He}}{dz} + \lambda M_{3He,z} \qquad (5)$$

where $M_{3He,z}$ denotes the total mass of ^{3}He (or ^{3}H) beneath depth z, dC_{3He}/dz is the concentration gradient of ^{3}He at depth z, and λ is the decay constant of ^{3}H.

Because of the strong and stable vertical gradients of ^{3}He in the intermediate depth range and its regular long-term behavior (Fig. 4C), ^{3}He is better suited to derive K_z estimates over long time periods than temperature. In particular, the ^{3}He profiles do not exhibit changes of sign of the vertical gradient, except for a few fluctuations within

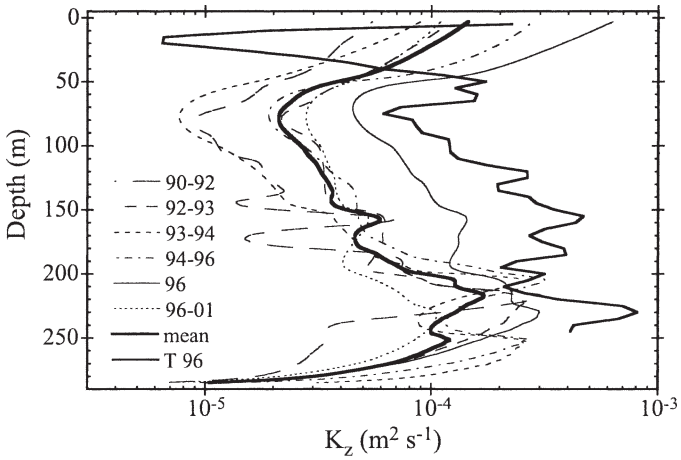

Fig. 10. K_z profiles calculated by the budget gradient meth od applied to ^{3}He (Eq. 5) for the periods between successive samplings and a weighted mean thereof. A K_z profile obtained from the temperature budget (Eq. 4) for the summer of 1996 is also shown.

experimental error in the deepest part. After elimination of one point in each of the ^{3}He profiles from 1990, 1992, and 1993, all ^{3}He and ^{3}H profiles were interpolated, and total tracer masses as well as vertical gradients at intervals of $\Delta z = 1$ m were calculated from the interpolated profiles. Using these data, K_z was then calculated by solving Eq. 5 for each interval between two tracer samplings. The resulting K_z profiles smoothed by a running mean over 5 m-bins are shown in Fig. 10, together with a mean profile calculated by weighting the results of the different intervals according to their duration. A K_z profile calculated from the temperature profiles of March and September 1996 is also shown in Fig. 10.

The mean K_z profile shows a minimum of about 2×10^{-5} m^2 s^{-1} at a depth of 80 m and a maximum that is higher by an order of magnitude at about 200 m in depth. The shape of the profile in the deep water is more or less inverse to the profile of N^2 (Fig. 6), as expected, since a stronger stratification should lead to less turbulent mixing. The profiles from most intervals are similar to the mean profile, except for substantially lower K_z values for the periods ranging from 1990 to 1992 and 1993 to 1994 and the higher values for the short period in the summer of 1996. An exceptionally strong vertical mixing between March and September 1996 is also supported by the even higher K_z profile derived from the temperature data.

The K_z values derived from the budget-gradient method can only be interpreted as realistic measures of turbulent diffusion if this is the dominant transport process. The upper part of the water column is of course also affected by seasonal convection. In the deep water, the calculated K_z values should at least give an indication of the overall strength of the water exchange, even if nondiffusive processes likely do contribute. In this sense, our results may be seen as "effective" K_z values.

A second way to derive information on the rate of deep-water renewal in the lake from the time series of ^{3}H and ^{3}He data is by simple box model calculations. If we

Table 3. Results of two box calculations (s, shallow; d, deep; box boundary at 100 m in depth).

Date	Mean concentrations (TU) and ages (yr) in boxes*							Exchange rate (yr $^{-1}$)		
	^3H_s	^3H_d	^3He_s	^3He_d	τ_s	τ_d	$\Delta\tau$	Period	$k_{ex,He}$†	$k_{ex,\tau}$†
May 90	37.7	47.0	40.1	84.0	5.3	14.3	9.0	1990 1992	0.033	0.023
Dec 92	30.4	40.5	39.7	86.4	6.1	16.2	10.1	1992 1993	0.090	0.044
Oct 93	28.1	37.8	38.8	84.6	5.9	16.7	10.8	1993 1994	0.034	0.028
Sep 94	26.4	35.9	38.0	85.1	8.1	17.3	9.2	1994 1996	0.080	0.069
Mar 96	23.6	33.1	37.7	82.5	6.1	17.7	11.6	Mar Sep 1996	0.192	0.024
Sep 96	22.9	30.0	36.4	78.9	6.1	18.1	12.0	1996 2001	0.091	0.042
May 01	15.0	20.0	34.5	69.1	7.7	20.4	12.7	1990 2001‡	0.077‡	0.039‡

* Volume weighted mean of the ^{3}He and ^{3}H concentrations and apparent ^{3}H ^{3}He ages τ from interpolated profiles, subscripts denote surface (*s*) and deep water (*d*). ^{3}He values are total concentrations; the tritiogenic component is lower by ~25.2 tritium units (TU).
† $k_{ex,He}$ calculated from the ^{3}He balance (Eq. 6); $k_{ex,\tau}$ calculated from the age balance (Eq. 7).
‡ Exchange rates for the entire period calculated as weighted mean of the rates for subperiods.

consider a two-box model of the lake, where the upper box represents the seasonally mixed shallow water and the lower box the permanently stratified deep water, the ^{3}He mass balance for the deep water can be written as

$$\frac{dC_{3He,d}}{dt} = k_{ex}(C_{3He,s} - C_{3He,d}) + \lambda C_{3H,d} \qquad (6)$$

where C denotes the concentrations of the tracers in the respective boxes (indices d for deep and s for shallow water) and k_{ex} is the exchange rate of the deep water ($k_{ex} = Q_{ex}/V_d$, when Q_{ex} is the water volume that is exchanged between the two boxes per year).

For box model calculations in Lake Lugano, the boundary between the shallow and deep boxes was chosen at a depth of 100 m, which is the lower boundary of the seasonally mixed zone. The concentrations in the two boxes were calculated from the ^{3}H and ^{3}He profiles, and the exchange rate k_{ex} was then derived from Eq. 6 for periods between two successive samplings. The results are listed in Table 3.The mean exchange rate over the entire study period from 1990 to 2001 is about 8% per year (averaging the exchange rates for the individual periods weighted with the durations of the periods yields $k_{ex} = 0.077$ yr $^{-1}$, whereas applying Eq. 6 directly to the data from 1990 and 2001 yields $k_{ex} = 0.082$ yr $^{-1}$). The periods 1990 1992 and 1993 1994 give lower exchange rates of only about 0.03 yr $^{-1}$. In contrast, the short summer period between March and September 1996 yields a high exchange rate of 0.19 yr $^{-1}$ (with a comparatively high uncertainty estimated at $\pm$0.05 yr $^{-1}$ because of the short interval). This pattern reflects of course the low and high K_z values derived above from the same data. There may be an increasing trend in the exchange rates over the study period, but the fluctuations are large.

The mean exchange rate of 0.08 yr $^{-1}$ implies a mean deep-water residence time $\tau = V_d/Q_{ex}$ of 12 13 yr for Lake Lugano. It is tempting to estimate this mean residence time directly from the differences $\Delta\tau = \tau_d \quad \tau_s$ of the mean apparent ^{3}H-^{3}He ages of the deep and shallow water, which indeed lie in a similar range between 9 and 13 yr (Table 3). However, this simple approach is not strictly correct. On the one hand, the apparent tracer ages deviate from the true mean residence time, as discussed above; on the other hand, even the true age difference would only equal the inverse of the exchange rate if steady-state conditions prevailed. The apparent age of the deep water is not at steady state, as the increase from 14 yr in 1990 to 20 yr in 2001 shows (Table 3). If the apparent age τ changes over time, the exchange rate has to be calculated from a balance equation similar to Eq. 6 with a source term for the age of 1 (increase of 1 yr yr $^{-1}$). Solved for k_{ex} this yields (Aeschbach-Hertig 1994):

$$k_{ex} = \frac{1 - d\tau_d/dt}{(\tau_d - \tau_s)} \qquad (7)$$

The age balance (Eq. 7) yields lower exchange rates than the tracer balance (Eq. 6), with a mean of only 4% per year (Table 3). These results are considered to be unreliable because in contrast to the tracer mass, the apparent age is not conserved in the exchange process. The mixed-reactor model discussed above motivates a simple approximating explanation for the different exchange rates obtained from Eqs. 6 and 7. This explanation assumes that the true long-term mean deep-water exchange rate is about 8% per year, as indicated by the ^{3}He balance, and the true mean deep-water residence time is roughly at steady state. As a result of the nonlinear effects of mixing on the ^{3}H-^{3}He age, the apparent age τ_d is not constant but increases at a rate of about $d\tau_d/dt \sim 0.5$ (the exact value between 1990 and 2001 was 0.56). This mostly artificial age increase reduces the result of Eq. 7 to about half of the steady-state value.

In summary, the ^{3}H-^{3}He mass-balance calculations show that there is considerable deep-water exchange in Lake Lugano, which can be characterized by effective K_z values of the order of 10^{-5} to 10^{-4} m^2 s $^{-1}$ at 100 m in depth (Fig. 10) or an exchange rate of about 8% per year for the deep water below this depth (Table 3). These values are long-term means for the entire study period. For shorter intervals, the deep-water exchange rate seems to fluctuate strongly, possibly because of the influence of discrete mixing events. The exchange rates obtained for single intervals may indicate a trend of increasing mixing, whereas the increasing ^{3}H-^{3}He ages would seem to argue for a decreasing mixing efficiency. However, this apparent

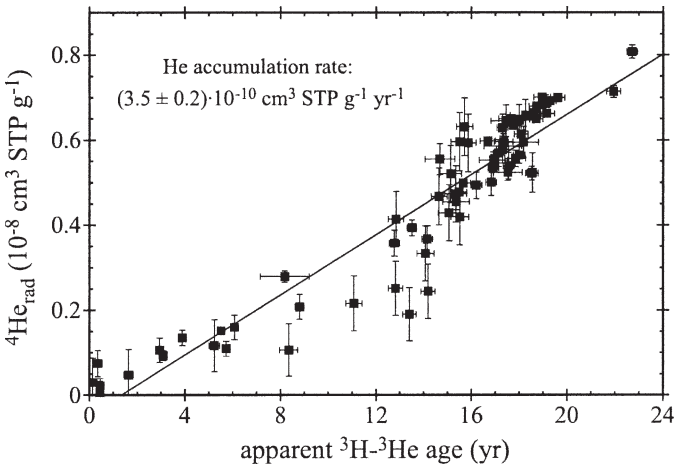

Fig. 11. Correlation of the excess of radiogenic ^{4}He with apparent ^{3}H ^{3}He ages. All data of the observation period are shown. The slope of the regression line yields an estimate of the accumulation rate of radiogenic He in the lake.

age increase is likely, at least in part, to be an artefact of the nonlinear behavior of the ^{3}H-^{3}He age.

^{4}He accumulation The apparent ^{3}H-^{3}He ages can be used to derive a first-order estimate of the accumulation rate of radiogenic He in the lake by a linear correlation of the concentrations of radiogenic ^{4}He with the ^{3}H-^{3}He ages. In Lake Lugano the ^{4}He excess correlates well ($R^2 = 0.89$) with the ^{3}H-^{3}He age over the entire observation period (Fig. 11). The slope of the correlation line yields an accumulation rate of radiogenic ^{4}He of $(3.5 \pm 0.2) \times 10^{-10}$ cm^3 STP g^{-1} yr^{-1}. Multiplying this rate with the mean depth of the basin yields an estimate of the ^{4}He flux F_{He}, which is assumed to be uniform over the entire sediment area. The result of $F_{He} = (6.0 \pm 0.3) \times 10^{-2}$ cm^3 STP m^{-2} yr^{-1} = $(5.1 \pm 0.3) \times 10^{10}$ atoms m^{-2} s^{-1} is a factor of two to three higher than in comparable perialpine lakes of northern Switzerland (Lake Zug: Aeschbach-Hertig 1994; Lake Lucerne: Aeschbach-Hertig et al. 1996). On the other hand, it is lower by a similar factor than fluxes derived by the same method in one basin of Lake Lucerne (Urnersee: Aeschbach-Hertig et al. 1996) and in Lake Baikal (Hohmann et al. 1998). The high He fluxes in these latter cases have been explained by inflow of groundwater, which can have very high He concentrations and can thus increase the total He flux into a lake.

Interestingly, the estimate of the crustal He flux in Lake Lugano agrees reasonably well with theoretical estimates of the average He flux from the continental crust of about 3×10^{10} atoms m^{-2} s^{-1} (O'Nions and Oxburgh 1983; Torgersen and Ivey 1985). He fluxes observed in other lakes are of the same order of magnitude, although they vary considerably (Kipfer et al. 2002). Yet while lakes are suitable to determine modern local He fluxes and their variability, they may not be ideal to test the hypothesis of a whole crustal He flux (Torgersen and Clarke 1985) on large temporal and spatial scales.

Furthermore, the method used above to estimate the He flux may lead to a biased result for two reasons (Kipfer et al. 2002). The first problem is that the radiogenic ^{4}He originates from the sediment area, whereas the tritiogenic ^{3}He and, hence, the apparent ^{3}H-^{3}He age are produced approximately uniformly throughout the water column. Because the ratio of sediment area to water volume increases with depth in a lake, the ratio of the radiogenic ^{4}He to the apparent ^{3}H-^{3}He age should also increase in the deepest part of the lake. In fact, in Fig. 11, a stronger-than-average increase of ^{4}He with age may be seen for ages between about 13 and 18 yr, but not for the highest ages corresponding to the deepest layers. Possibly boundary mixing obscures the expected effect of lake geometry near the lake bottom. The second problem is that the apparent ^{3}H-^{3}He age may deviate systematically from the true mean residence time of the deep water, as discussed above. The only strict way to solve the problem seems to be inverse fitting of the He concentrations using a one-dimensional vertical lake model with F_{He} as a fit parameter, as demonstrated by Aeschbach-Hertig et al. (2002). Using such a model and assuming that the 1992 He profile from Lake Lugano was at steady state, Aeschbach-Hertig (1994) derived a value for F_{He} of $(3.5 \pm 0.3) \times 10^{10}$ atoms m^{-2} s^{-1}, somewhat lower than the above estimate from the simple regression method.

The assumption of a steady-state He profile in 1992 was not strictly correct, since our data series reveals a slow increase of the concentrations in the deep water (Fig. 4B). This continuous increase of He concentrations indicates that a balance between He input from the sediments and He removal by vertical mixing has not yet been reached. Assuming the He flux is constant over time, the He increase in the deep water could indicate either the slow approach to a new steady state after a reduction of the deep-water renewal rate in the past or an ongoing slight reduction of this rate during the observed period.

Implications for the mixing dynamics Our time series of transient tracer and CTD profiles provides some insight into the evolution of the mixing dynamics of Lake Lugano. The salinity-induced density stratification remained nearly unchanged throughout the observed period of 1990 to 2001 (Fig. 3B). The persisting increase of conductivity with depth indicates a continuous flux of dissolved ions from the sediments toward the surface. The origin of this flux is mineralization of settling organic matter (Wüest et al. 1992), which apparently remained high despite successful efforts to reduce the external nutrient load to the lake. Because the salinity gradient decisively controls the stability of the deep water, a reduction of this flux appears to be necessary to reduce the density stratification and to allow regular deep-reaching mixing.

However, the stratification was also weakened by the continuous increase of the deep-water temperature. This warming was mainly due to a turbulent diffusive flux from above and the geothermal heat flow from below. Winter convection was too weak to reset the warming during our observation period. The increasing deep-water temperature has lowered the density of the deep water to the point where a sufficiently cold winter could create an instability of the water column despite the stabilizing salinity gradient.

However, the warming climate reduced the probability of such an event, which did not occur until the cold and windy winter of 2004 2005.

During our observation period, the CTD data reveal no clear changes in the strength of the vertical mixing. The apparent water ages obtained from transient tracers only roughly reflect the mean residence time of the deep water and, hence, are difficult to interpret with regard to changes of the mixing intensity. In particular, the increase of the apparent ^{3}H-^{3}He age of the deep water from about 14 yr in 1990 to 20 yr in 2001 does not necessarily indicate decreasing mixing or an approach to a steady state with very low deep-water renewal. A simple mixed-reactor model as well as the analysis of the evolution of the ^{3}H and ^{3}He concentrations in the deep water show that this increase could be consistent with a more or less constant deep-water exchange rate of about 8% per year. The observed increase of the apparent ^{3}H-^{3}He age as well as the large deviation from the SF_6 age may to a large extent be an artefact caused by the nonlinearity of the ^{3}H-^{3}He age. The apparent SF_6 age of 10 12 yr in the deep water likely underestimates the true mean residence time, but may be closer to reality than the 20-yr value indicated by the ^{3}H-^{3}He method.

These results show that it is not advisable to use apparent tracer ages to estimate exchange rates in lakes, at least in cases involving relatively high ages. A much better way to estimate the deep-water exchange rate and its change over time is to calculate mass balances of the ^{3}H and ^{3}He concentrations between consecutive samplings. For Lake Lugano, such calculations using a two-box model result in exchange rates varying from 0.03 yr $^{-1}$ to 0.19 yr $^{-1}$, with an average value of 0.08 yr $^{-1}$ for the deep water below 100 m in depth. The results for the individual periods scatter too strongly to clearly identify a possible trend toward weaker mixing. Such a trend would, however, also be consistent with the ongoing slow accumulation of radiogenic ^{4}He in the deep water.

Despite the shortcomings of the apparent tracer ages as a result of the effects of mixing, the large data set presented here provides an estimate of the deep-water renewal in Lake Lugano during the observation period, which may serve as a reference for the assessment of the recent and future evolution of this strongly anthropogenically influenced lake system. In the absence of older tracer data and a detailed modeling of the long-term evolution of the tracer concentrations, we cannot make an unequivocal statement on the evolution of the mixing intensity since the onset of meromixis in the 1960s. However, the simple assumption that the deep-water exchange rate remained on average constant over several decades at a level of about 8% per year appears to explain our data quite well. Wüest et al. (1992) showed that the vertical density structure observed in 1990 was consistent with a steady state resulting from the balance of vertical turbulent mixing and geothermal heat flow and mineralization at depth. Our data show that such approximately constant conditions have persisted throughout the 1990s, and it is likely that they had already existed in at least the two prior decades. Only recently, possibly facilitated by the slow warming of the deep water, has a dramatic change in the mixing regime occurred which is, however, not the issue of this paper.

References

Aeschbach Hertig, W. 1994. Helium und Tritium als Tracer für physikalische Prozesse in Seen. Diss. ETH Nr. 10714. Ph.D. thesis, ETH Zürich.

, M. Hofer, M. Schmid, R. Kipfer, and D. M. Imboden. 2002. The physical structure and dynamics of a deep, meromictic crater lake (Lac Pavin, France). Hydrobiology **487:** 111 136.

, R. Kipfer, M. Hofer, D. M. Imboden, and H. Baur. 1996. Density driven exchange between the basins of Lake Lucerne (Switzerland) traced with the ^{3}H ^{3}He method. Limnol. Oceanogr. **41:** 707 721.

, F. Peeters, U. Beyerle, and R. Kipfer. 1999. Interpretation of dissolved atmospheric noble gases in natural waters. Water Resour. Res. **35:** 2779 2792.

Barbieri, A., and R. Mosello. 1992. Chemistry and trophic evolution of Lake Lugano in relation to nutrient budget. Aquat. Sci. **54:** 219 237.

, and B. Polli. 1992. Description of Lake Lugano. Aquat. Sci. **54:** 181 183.

, and M. Simona. 2001. Trophic evolution of Lake Lugano related to external load reduction: Changes in phosphorus and nitrogen as well as oxygen balance and biological parameters. Lakes Reserv. Res. Manage. **6:** 37 47.

Begert, M., T. Schlegel, and W. Kirchhofer. 2005. Homogeneous temperature and precipitation series of Switzerland from 1864 to 2000. Int. J. Climatol. **25:** 65 80.

Benson, B. B., and D. Krause. 1980. Isotopic fractionation of helium during solution: A probe for the liquid state. J. Solution Chem. **9:** 895 909.

Beyerle, U., W. Aeschbach Hertig, D. M. Imboden, H. Baur, T. Graf, and R. Kipfer. 2000. A mass spectrometric system for the analysis of noble gases and tritium from water samples. Environ. Sci. Technol. **34:** 2042 2050.

Bullister, J. L., D. P. Wisegarver, and F. A. Menzia. 2002. The solubility of sulfur hexafluoride in water and seawater. Deep Sea Res. I **49:** 175 187.

Busenberg, E., and N. L. Plummer. 2000. Dating young groundwater with sulfur hexafluoride: Natural and anthropogenic sources of sulfur hexafluoride. Water Resour. Res. **36:** 3011 3030.

Campbell, P., and T. Torgersen. 1980. Maintenance of iron meromixis by iron redeposition in a rapidly flushed monimolimnion. Can. J. Fish. Aquat. Sci. **37:** 1303 1313.

Clarke, W. B., W. J. Jenkins, and Z. Top. 1976. Determination of tritium by mass spectrometric measurement of ^{3}He. Int. J. Appl. Radiat. Isotopes **27:** 515 522.

DRP (Division of Radiation Protection). 1994 2006. Environmental radioactivity and radiation exposure in Switzerland. Yearly reports 1994 2005. Swiss Federal Office of Public Health, Bern.

Finckh, P. 1981. Heat flow measurements in 17 peralpine lakes: Summary. Geol. Soc. Am. Bull. I **92:** 108 111.

Ho, D. T., and P. Schlosser. 2000. Atmospheric SF_6 near a large urban area. Geophys. Res. Lett. **27:** 1679 1682.

Hofer, M., and D. M. Imboden. 1998. Simultaneous determination of CFC 11, CFC 12, N_2 and Ar in water. Anal. Chem. **70:** 724 729.

, and others. 2002. Rapid deep water renewal in Lake Issyk Kul (Kyrgyzstan) indicated by transient tracers. Limnol. Oceanogr. **47:** 1210 1216.

HOHMANN, R., M. HOFER, R. KIPFER, F. PEETERS, AND D. M. IMBODEN. 1998. Distribution of helium and tritium in Lake Baikal. J. Geophys. Res. **103:** 12823 12838.

IAEA (INTERNATIONAL ATOMIC ENERGY AGENCY). 1992. Statistical treatment of data on environmental isotopes in precipitation. International Atomic Energy Agency: Vienna,

. 2006. Use of chlorofluorocarbons in hydrology: A guide book. International Atomic Energy Agency: Vienna,

IAEA/WMO. 2004. Global network of isotopes in precipitation. The GNIP database [Internet]. Available from http://isohis.iaea.org. Accessed 14 Dec. 2004.

IMBODEN, D. M., AND A. WUEST. 1995. Mixing mechanisms in lakes, p. 83 138. *In* A. Lerman, D. M. Imboden and J. R. Gat [eds.], Physics and chemistry of lakes. Springer.

JASSBY, A., AND T. POWELL. 1975. Vertical patterns of eddy diffusion during stratification in Castle Lake, California. Limnol. Oceanogr. **20:** 530 543.

JENKINS, W. J., AND W. B. CLARKE. 1976. The distribution of ^{3}He in the western Atlantic Ocean. Deep Sea Res. **23:** 481 494.

KIPFER, R., AND OTHERS. 1996. Bottomwater formation due to hydrothermal activity in Frolikha Bay, Lake Baikal, eastern Siberia. Geochim. Cosmochim. Acta **60:** 961 971.

, , F. PEETERS, AND M. STUTE. 2002. Noble gases in lakes and ground waters, p. 615 700. *In* D. Porcelli, C. Ballentine and R. Wieler [eds.], Noble gases in geochemistry and cosmochemistry. Rev. Mineral. Geochem. Mineralogical Society of America, Geochemical Society.

LAVELLI, A., G. DE CESARE, AND J. L. BOILLAT. 2002. Modélisation des courants de turbidité dans le bassin nord du lac de Lugano. Laboratoire de constructions hydrauliques, Ecole Polytechnique Fédérale de Lausanne.

LIVINGSTONE, D. M. 1997. An example of the simultaneous occurrence of climate driven''sawtooth'' deep water warming/cooling episodes in several Swiss lakes. Verh. Int. Ver. Limnol. **26:** 822 828.

LSA (LABORATORIO STUDI AMBIENTALI). 1981 2000. Ricerche sull' evoluzione del Lago di Lugano; aspetti limnologici. Campagne annuali 1980 1999. Commissione Internazionale per la Protezione delle Acque Italo Svizzere [ed.].

, 1998. Ricerche sull' evoluzione del Lago di Lugano aspetti limnologici. p. Programma quinquennale 1993 1997. Commissione Internazionale per la Protezione delle Acque Italo Svizzere [ed.].

LUCAS, L. L., AND M. P. UNTERWEGER. 2000. Comprehensive review and critical evaluation of the half life of tritium. J. Res. Natl. Inst. Stand. Technol. **105:** 541 549.

MAMYRIN, B. A., AND I. N. TOLSTIKHIN. 1984. Helium isotopes in nature, 1st ed. Elsevier.

MARTY, B., R. K. O'NIONS, E. R. OXBURGH, D. MARTEL, AND S. LOMBARDI. 1992. Helium isotopes in Alpine regions. Tectonophysics **206:** 71 78.

O'NIONS, R. K., AND E. R. OXBURGH. 1983. Heat and helium in the earth. Nature **306:** 429 431.

PEETERS, F., AND OTHERS. 2000. Analysis of deep water exchange in the Caspian Sea based on environmental tracers. Deep Sea Res. I **47:** 621 654.

, , R. HOHMANN, M. HOFER, D. M. IMBODEN, G. G. KODENEV, AND T. KHOZDER. 1997. Modelling transport rates in Lake Baikal: Gas exchange and deep water renewal. Environ. Sci. Technol. **31:** 2973 2982.

REICHERT, P. 1994. AQUASIM a tool for simulation and data analysis of aquatic systems. Water Sci. Technol. **30:** 21 30.

SCHLOSSER, P., AND G. WINCKLER. 2002. Noble gases in the ocean and ocean floor. *In* D. Porcelli, C. Ballentine and R. Wieler [eds.], Noble gases in cosmochemistry and geochemistry. Rev. Mineral. Geochem. Mineralogical Society of America, Geochemical Society.

SPAAS (SEZIONE PROTEZIONE ARIA, ACQUA E SUOLO). 2005. Stato limnologico del Lago di Lugano: Circolazione invernale 2004 2005. Bollettino dei laghi Maggiore e Lugano. No. 6 Luglio 2005. Commissione Internazionale per la Protezione delle Acque Italo Svizzere [ed.].

TORGERSEN, T., AND W. B. CLARKE. 1985. Helium accumulation in groundwater, I: An evaluation of sources and the continental flux of crustal ^{4}He in the Great Artesian Basin, Australia. Geochim. Cosmochim. Acta **49:** 1211 1218.

, , AND W. J. JENKINS. 1979. The tritium/helium 3 method in hydrology, p. 917 930. *In* IAEA [ed.], Isotope hydrology 1978. IAEA.

, D. E. HAMMOND, W. B. CLARKE, AND T. H. PENG. 1981. Fayetteville, Green Lake, New York: ^{3}H ^{3}He water mass ages and secondary chemical structure. Limnol. Oceanogr. **26:** 110 122.

, AND G. N. IVEY. 1985. Helium accumulation in groundwater, II: A model for the accumulation of the crustal ^{4}He degassing flux. Geochim. Cosmochim. Acta **49:** 2445 2452.

, Z. TOP, W. B. CLARKE, W. J. JENKINS, AND W. S. BROECKER. 1977. A new method for physical limnology tritium helium 3 ages results for Lakes Erie, Huron and Ontario. Limnol. Oceanogr. **22:** 181 193.

VOLLMER, M. K., R. F. WEISS, P. SCHLOSSER, AND R. T. WILLIAMS. 2002. Deep water renewal in Lake Issyk Kul. Geophys. Res. Lett. **29:** 1283, doi:10.1029/2002GL014763.

WAUGH, D. W., M. K. VOLLMER, R. F. WEISS, T. W. N. HAINE, AND T. M. HALL. 2002. Transit time distributions in Lake Issyk Kul. Geophys. Res. Lett. **29:** 2231, doi:10.1029/2002GL016201.

WEISS, R. F. 1971. Solubility of helium and neon in water and seawater. J. Chem. Eng. Data **16:** 235 241.

, E. C. CARMACK, AND V. M. KOROPALOV. 1991. Deep water renewal and biological production in Lake Baikal. Nature **349:** 665 669.

WUEST, A., W. AESCHBACH HERTIG, H. BAUR, M. HOFER, R. KIPFER, AND M. SCHURTER. 1992. Density structure and tritium helium age of deep hypolimnetic water in the northern basin of Lake Lugano. Aquat. Sci. **54:** 205 218.

Received: 22 March 2006
Accepted: 22 September 2006
Amended: 29 September 2006